Turkish Journal of Electrical Engineering & Computer Sciences

http://journals.tubitak.gov.tr/elektrik/

Research Article

Turk J Elec Eng & Comp Sci
(2016) 24: 5025 – 5042

doi:10.3906/elk-1409-92

A new algorithm for avoiding maloperation of transformer restricted earth fault protection caused by the transformer magnetizing inrush current and current transformer saturation

Jelisaveta KRSTIVOJEVIC*, Milenko DJURIC
University of Belgrade-School of Electrical Engineering, Belgrade, Serbia

Received: 14.09.2014 • **Accepted/Published Online:** 25.10.2015 • **Final Version:** 06.12.2016

Abstract: Owing to current transformer (CT) saturation caused by a decaying direct current component in the magnetizing inrush current, the restricted earth fault (REF) protection of a power transformer could maloperate during magnetizing inrush. This paper presents a new transformer restricted earth fault relay algorithm that can prevent false relay tripping and provide proper action during the energization of a faulty transformer. The integral of the product of the signals that are compared is calculated over 1 half-period of the signals. The performance of the proposed algorithm is tested and verified using a large number of transformer energization trials and fault cases. The signals required for testing of the algorithm were obtained by laboratory measurements, and then the algorithm was tested off-line. The influence of different levels of CT saturation due to different remanent fluxes in CT cores during power transformer energization was investigated. By applying computer simulations, the signals required for algorithm testing were generated. The investigation results presented in this paper show that the new algorithm provided sensitive protection for the power transformer for phase to ground faults and high security and stability during magnetizing inrush conditions in conjunction with CT saturation.

Key words: Power transformer protection, restricted earth fault protection, magnetizing inrush, current transformer saturation, digital phase comparison

1. Introduction

A transformer is an exceptionally vital and expensive component of an electric power system. It is essential that a transformer is equipped with reliable, secure, and fast protection against possible internal faults. It is also quite important that the transformer protection system does not make false tripping. For protection systems of a power transformer it is essential to be able to distinguish internal faults from external disturbances capable of causing false tripping.

Phase differential protection is usually applied for the protection of power transformers. In many cases it provides a satisfactory level of reliability and safety. However, phase differential protection is not sufficiently sensitive for detecting an internal phase-to-ground fault if the fault is located near the neutral point of the transformer, or if the ground-fault current is limited [1]. The restricted earth fault (REF) protection is used as an additional protection method in order to overcome this problem [2–5].

A magnetizing inrush current severely affects the proper operation of transformer protection systems. It is well known that in the case of phase differential protection a magnetizing current causes the appearance of a

*Correspondence: j.krstivojevic@etf.rs

false differential current that may result in false tripping. Since applications of numerical differential protection began [6] up to the present date, different methods of protection improvement have been developed whereby the unfavorable influence of a magnetizing inrush current can be overcome. Some of them are wavelet transform [7–9], artificial neural network [10–14], fuzzy logic [15,16], S-transform [17,18], waveform analysis [6,19], and harmonic restraint and blocking [20,21]. Waveform analysis and harmonic restraint and blocking [2] are the most often applied.

When the performance of a power transformer protection system and its adjustment are considered, it is necessary to take into account current transformer (CT) saturation and its effect on protective relays [22–25]. Saturation of a protective CT cannot be totally eliminated despite proper dimensioning [10]. CT saturation is usually caused by a high amplitude of the fault current, due to the presence in the fault current of a slowly decaying direct circuit (DC) component, and by the remanent flux in the CT core.

It is known that the shape and amplitude of the magnetizing inrush current of a power transformer are dependent on several factors that cannot be predicted in advance. Magnetizing current contains a slowly decaying DC component and a significant level of even and odd harmonics. The presence of the slowly decaying DC component may lead to CT saturation, even at lower values of the current [26], while the worst CT saturation is caused by a DC component in the primary current [25,26].

High-impedance REF relays possess certain levels of immunity to CT saturation. The use of this relay requires some design considerations to be satisfied, such as the same number of turns ratios of the phase and neutral CTs, the same saturation characteristics, and closely similar and high knee-point voltage of the CTs [27]. Today, numerical low-impedance REF relays are widely used. A very important advantage of low-impedance REF protection is the fact that the CT's characteristics and ratios for the phase and neutral CTs do not have to be the same. However, if saturation of the CT is present during the no fault condition, a false differential current appears and this current is generally sufficient to cause a 'false' relay operation.

The operation of this relay can be improved by using harmonic restraint supervision methods [27,28], directional supervision [27,29], or adaptive restraint current methods [30]. This paper proposes a new method founded on the application of a directional function based on a time-domain digital phase comparator [31]. The new algorithm, presented in this paper, provides sensitive protection of the power transformer against phase to ground faults and offers high security and stability during magnetizing inrush conditions. Application of the new algorithm would result in avoiding unnecessary operations of REF relays during energizing of a power transformer accompanied by CT saturation. Moreover, the REF relay algorithm is complemented by the condition to ensure the proper operation of the relay during the energization of a faulty transformer.

Testing and verification of operation of the algorithm were carried out in 2 ways. Firstly, the operation of the proposed algorithm was tested by laboratory recorded signals for a number of different faults and transformer switch-ons. In the literature, the influence of saturation of only 1 individual CT is usually considered. In this work, tests of CT saturations in each of the 3 phases were covered. The second group of tests considered the influence of different levels of CT saturation on the operation of the algorithm owing to different remanent fluxes in the CT core. To this end, by using the MATLAB module Power Systems Blockset, a model was formulated and used for simulation of CT operation. Samples of laboratory recorded signals were used as primary current in the model. The secondary current generated by the simulations was used for testing the algorithm. In all tests carried out on the basis of laboratory measurements and performed simulations, it was shown that the proposed method was robust and suitable for application in cases of CT saturation.

2. The new method of avoiding malfunctioning of REF protection due to magnetizing inrush

2.1. Concept of REF protection

The REF relay operates for phase-to-ground faults of a grounded winding and also of the delta winding if a grounding transformer is installed between the delta winding and the CTs [27]. Operation of a REF relay is based on differential principle. The relay compares transformer neutral current with the sum of the phase currents and thereby makes a trip decision.

For ground faults outside a transformer (F1) and within a transformer (F2) the directions of the zero sequence currents through CT1 are the same, but the directions of the sums of the phase currents are opposite for the 2 mentioned faults (Figure 1). Therefore, the directional function can distinguish faults within a transformer from faults outside the transformer. The same applies for faults F3 and F4 at the delta-connected side.

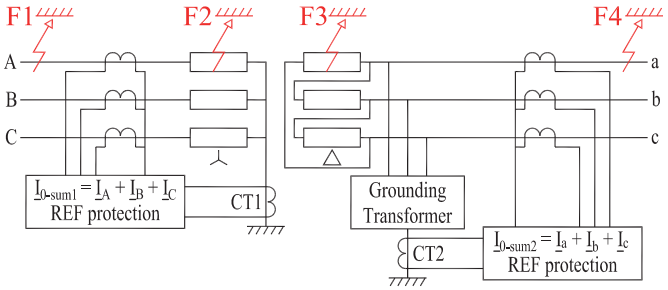

Figure 1. Transformer ground fault protection.

During magnetizing inrush REF protection should operate correctly. However, the presence of a slowly decaying DC component in the magnetizing current could easily bring one or more CT to deep saturation and thereby cause REF relay maloperation. Even though the inrush magnetizing current in power transformers is usually related to the switching on of unloaded transformers, it can be caused by sudden step-changes in the transformer magnetizing voltage and can be divided into 3 general types: initial inrush, recovery inrush, and sympathetic inrush. Since recovery inrush and sympathetic inrush will always be less than the initial inrush [32], testing of the algorithm in this paper will be carried out using initial inrush currents.

Saturation of CTs is difficult to predict. Even CTs with identical nominal parameters could reproduce the same fault current differently [26]. The unfavorable influence of CT saturation on the operation of relay protection can be twofold. During an internal fault, the presence of harmonics in the secondary current due to CT saturation may undesirably delay relay operation, while during an external fault CT saturation may cause the appearance of a false differential current [25].

In order to avoid false operation of the REF relay protection caused by CT saturation, the directional supervision methods combined with harmonic restraint and blocking due to the presence of a higher harmonic are often applied [27,28]. The second harmonic restraint method in the neutral current should ensure that the relay does not react unnecessarily during transformer switching on. However, with internal transformer faults the level of the second harmonic can be high [8,10,16,33]; thus in these situations the relay would have been unnecessarily blocked. It was noted that in the magnetizing inrush currents of the new generation transformers having cores made of low-loss amorphous materials, the contents of the second harmonic were considerably lower, whereas the current amplitudes could be quite high [8]. Furthermore, relay blocking by the second harmonic during magnetizing inrush may prevent proper operation of the relay when energizing a faulty transformer [28]. It is therefore advisable to apply a method that does not rely on higher harmonics content.

2.2. Basic concept of the application of a time-domain phase comparator in REF protection algorithm

The application of a time-domain digital phase comparator (DPC) in the proposed REF protection algorithm is based on the calculation of the average power of the signals on a half-cycle data window. This method has previously been proposed and applied [31,34,35]. In order to speed up the rate of convergence of the process of calculation of normalized integral value, the method of its calculation was modified [29].

Digital phase comparison of the 2 signals (i_{s1}) and (i_{s2}) is carried out by using the formula

$$DPC = \frac{2}{m}\sum_{n=1}^{m/2} i_{s1}(n)\cdot i_{s2}(n), \tag{1}$$

where m – even number of samples within signal period; DPC – average power of the 2 signals over 1 half period; $i_{s1}(n) - n$th sample of the signal i_{s1}; and $i_{s2}(n) - n$th sample of the signal i_{s2}.

Calculation of the root mean square (rms) indicators is carried out by using the expressions

$$I_{s1\_ind} = \sqrt{\frac{2}{m}\sum_{n=1}^{m/2} i_{s1}(n)\cdot i_{s1}(n)}, \tag{2}$$

$$I_{s2\_ind} = \sqrt{\frac{2}{m}\sum_{n=1}^{m/2} i_{s2}(n)\cdot i_{s2}(n)}. \tag{3}$$

The directional index that will be used for the phase comparison represents the normalized value of expression (1):

$$I_{DI} = DPC(p.u.) = \frac{DPC}{I_{s1\_ind}\cdot I_{s2\_ind}} \tag{4}$$

Consider a phase-to-ground fault (F1) at the wye side of the transformer shown in Figure 1. In the considered case, waveforms of the sum of phase currents at transformer terminals at the wye side ($3\,i_0$) and the neutral current (i_G) are shown in Figure 2a. It can be seen that currents ($3\,i_0$) and (i_G) are in phase; therefore DPC calculated by applying these 2 currents is positive. Figure 2b presents the case of an internal phase-to-ground fault (F2) at the wye side of the transformer. In this case phase shift between the current ($3\,i_0$) and neutral current (i_G) is approximately 180°; thus DPC is negative. Figures 3a and 3b show indicators of the rms values obtained by expressions (2) and (3) and directional index (equation 4) for external and internal phase-to-ground faults, respectively. For ground fault F1, currents i_{0-sum} and i_{0-G} are in phase; thus the value of the directional index is equal to 1 per unit (pu). For a ground fault F2 within a transformer, currents are mutually phase shifted by approximately 180°; thus the value of the directional index is approximately equal to -1 pu. The directional index is equal to the cosine of the angle (φ) that represents the phase shift between currents i_{0-sum} and i_{0-G}.

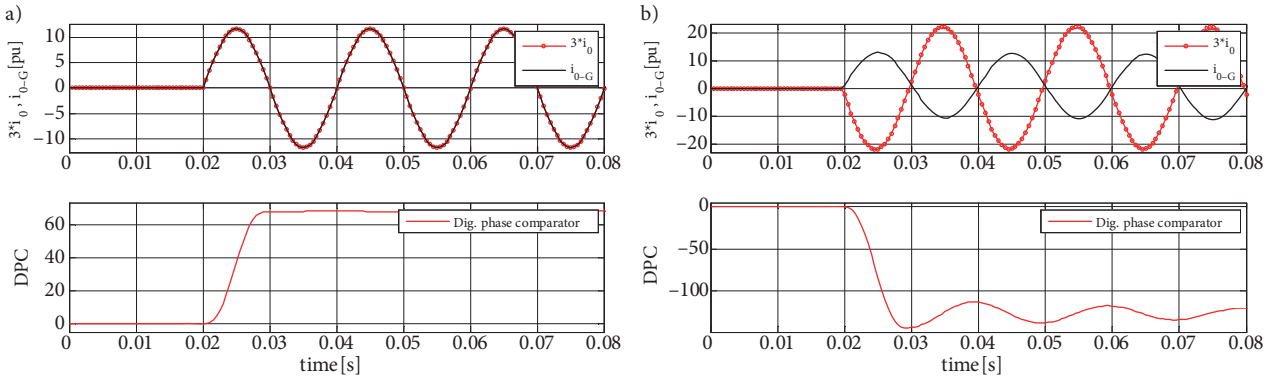

Figure 2. Currents $3i_0$ and i_G, and digital phase comparator: (a) external; (b) internal phase-to-ground fault.

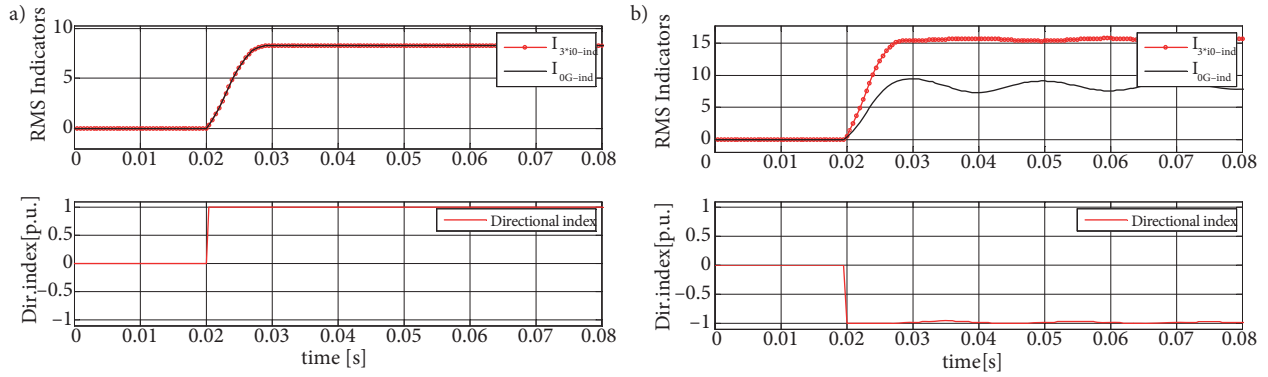

Figure 3. RMS Indicators and I_{DI} for phase-to-ground fault: (a) external, (b) internal.

2.3. The algorithm

This section presents an algorithm for REF protection. The REF relay algorithm is enhanced by adding conditions that ensure the proper operation of the relay during the energization of a faulty transformer. Based on the algorithm performance during tests presented in sections 3 and 4, definite tripping characteristic will be proposed and, in accordance with this discrimination stage in the algorithm, will be modified in section 5.

The input information to the algorithm is sampled values of the phase currents and transformer neutral current. The flow of the proposed algorithm for 1-winding REF unit, i.e. for a transformer high voltage winding, is as follows:

Step 1: Analogue to digital conversion of phase currents (i_A, i_B, and i_C) and transformer neutral current (i_N) with a preassigned sampling rate.

Step 2: Calculation of the following indicators. First, the sum of the phase currents and neutral current are given by expressions:

$$i_{0-sum}(k) = i_A(k) + i_B(k) + i_C(k), \tag{5}$$

$$i_{0-G}(k) = i_N(k). \tag{6}$$

Step 3: On the basis of expressions (2)–(4), calculation of the following indicators is carried out: $I_{0-sum}-$ rms indicator for (i_{0-sum}), $I_{0-G}-$ rms indicator for (i_{0-G}) and I_{DI} (pu) $-$ directional index.

Step 4: Testing if the value of indicator (I_{0-G}) is greater than the preassigned limiting value:

$$I_{\text{0-G}} > I_{TH}. \tag{7}$$

If this condition is fulfilled, the algorithm proceeds to the next step; otherwise it returns to step 1.

This step starts the detection phase. Condition (7) provides security as regards saturation of CT caused by external faults not involving contact with the ground, i.e. phase-to-phase and 3-phase faults. It is known that current will flow through the transformer neutral in the case of a ground fault; therefore it is suitable to introduce a condition ensuring operation of REF protection only if current in the transformer neutral exceeds a threshold value. The threshold value is selected to be higher than the zero current due to the load, CT mismatch, or any other imbalance.

Step 5: Testing if the rms indicator of the sum of currents is zero:

$$I_{\text{0-sum}} = 0. \tag{8}$$

This condition covers the case of energizing an unladen faulty power transformer containing a ground fault, the fault being at the open terminal's side of the transformer. E.g., consider energizing from the low voltage (LV) side of an unladen transformer containing a phase-to-ground fault at the high voltage (HV) side. Since HV terminals are open, the sum of the phase currents is equal to zero. However, owing to the presence of a phase-to-ground fault a current will flow through the neutral CT. Conditions (7) and (8) ensure proper functioning of the algorithm in these cases.

If condition (8) in step 5 is satisfied, it is considered that an internal ground fault is present; otherwise the algorithm proceeds to step 6.

Step 6: In this step the value of directional index I_{DI} is compared with the threshold value I_{DI_TH}.

$$I_{DI} \leq I_{DI\_TH} \tag{9}$$

The operation area can be reduced or enlarged as required by choosing the threshold value of directional index (I_{DI_TH}). The value of I_{DI_TH} should be chosen so that there will be no undesired tripping due to heavily saturated CT. If condition (9) is satisfied, it is considered that the present ground fault is within the protected zone.

Step 7: If conditions (7) and (9) or (7) and (8) are met, it is possible that an internal ground fault is present, the logic output is equal to 1, and trip signal is activated. Otherwise the logic output is equal to 0 and the algorithm returns to the start.

The algorithm steps are described for the high voltage winding. The tripping decision is formed in the same way for the low voltage transformer winding. The complete flow chart of the algorithm is shown in Figure 4.

3. The results of testing of the algorithm

Performance of the algorithm was tested by using signals obtained by experimental measurements. Test studies were carried out by using a custom-built transformer in the laboratory. The custom-built 3-phase transformer 5.8 kV/220 V was equipped with taps placed at the 25%, 50%, and 75% of the high voltage winding so that different internal faults could be generated. The transformer had a 3-limb core and YNyn connected windings.

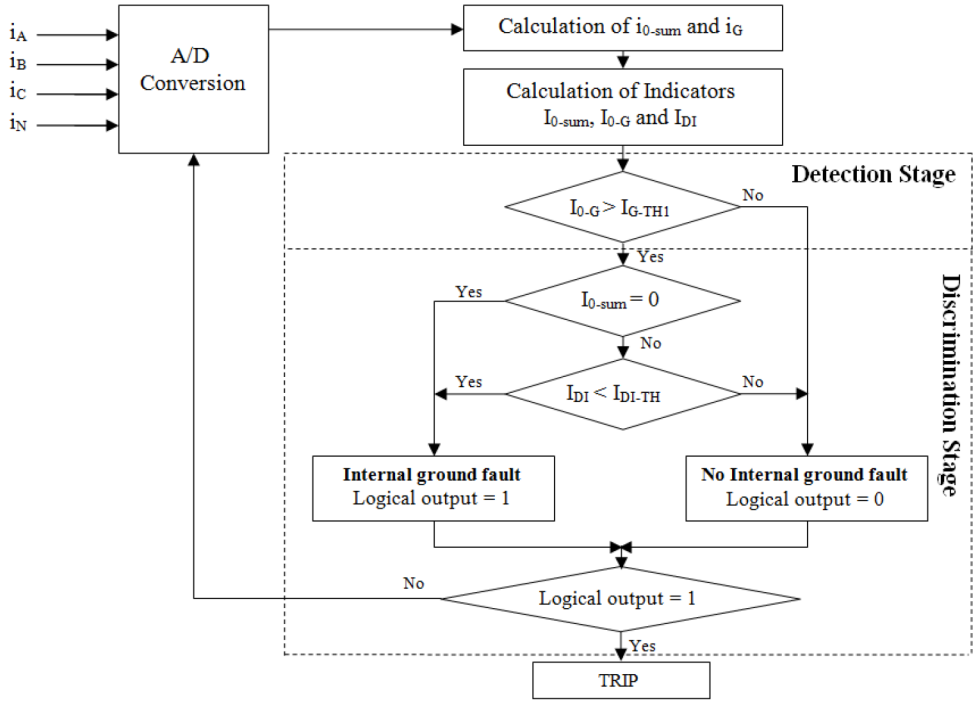

Figure 4. Flow chart of the algorithm.

A series of laboratory measurements was carried out with the aim of obtaining signals suitable for testing the algorithm. Figures 5, 6a, and 6b show the circuit diagrams used for these measurements. Recording and sampling of the currents were performed in real time by using a data acquisition system NI USB-6009. By applying the recorded signal samples, operation of the algorithm was tested off-line. Some of the energization and fault cases are listed in Table 1. In this table, cases 1 and 2 are magnetizing inrush cases, cases 3 through 9 are energization cases with internal faults, cases 10 through 15 are internal faults applied to loaded transformers, and cases 16 through 18 are external faults.

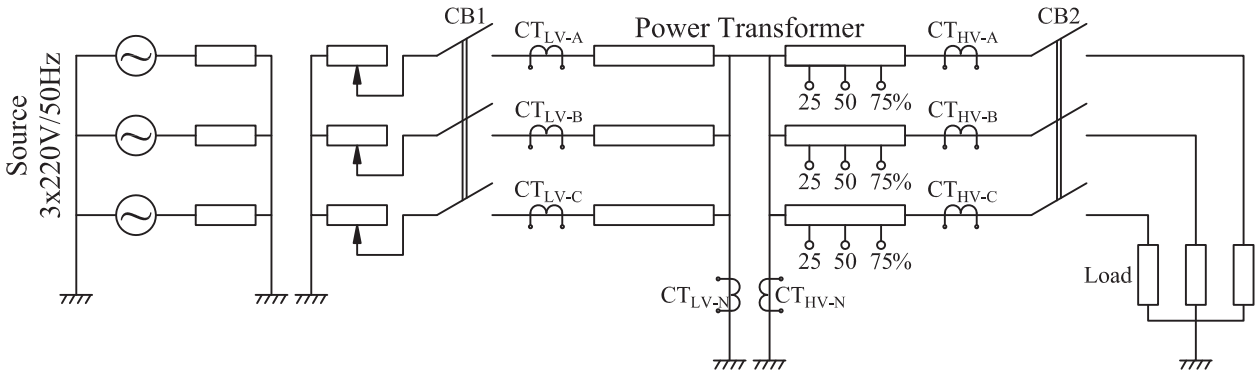

Figure 5. Circuit diagram for the experimental laboratory measurements.

In all examples presented, the calculated value of the directional index is compared with the threshold value $I_{DI\_TH} = -0.707$. If condition (9) is satisfied, phase shift (φ) is within the following limits: $\angle(i_{0-sum}, \cdot i_{0-G}) = \phi$, $135^\circ \leq \phi \leq 225^\circ$. In this case it is considered that the present ground fault is within the protected zone.

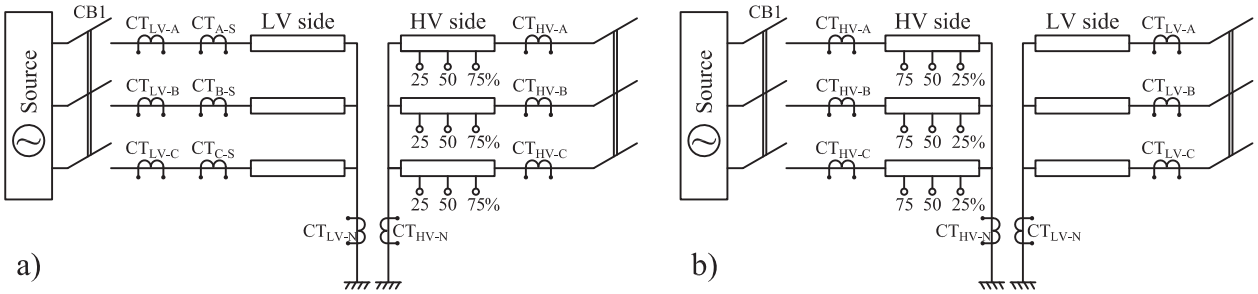

Figure 6. Energization of unloaded power transformer from: (a) low voltage side; (b) high voltage side.

Table 1. List of energization and fault studies.

Case	
Energization of unloaded power transformer (PT)	
1	Magnetizing inrush without current transformer saturation
2	Magnetizing inrush with current transformer saturation
Energization with internal fault	
- Fault on high voltage side, PT energized on high voltage side	
3	Phase A to G – 25% of high voltage wind.
4	Phase A to G – 50% of high voltage wind.
5	Phase A to G – 75% of high voltage wind.
- Fault on high voltage side, PT energized on low voltage side	
6	Phase A to G – 25% of high voltage wind.
7	Phase A to G – 50% of high voltage wind.
8	Phase A to G – 75% of high voltage wind.
9	Phase A to G – 100% of high voltage wind.
Internal fault – phase B to ground (G)	
10	25% of high voltage wind.
11	50% of high voltage wind.
12	75% of high voltage wind.
13	100% of high voltage wind.
14	50% of high voltage wind with current transformer saturation of phase B.
15	50% of high voltage wind. with neutral current transformer saturation
External fault – phase A to ground	
16	Without current transformer saturation
17	With current transformer saturation of phase A
18	With neutral current transformer saturation

3.1. Magnetizing inrush

A 3-phase transformer 5.8 kV/220 V is switched on by breaker CB1 to alternating voltage 3 $\times$ 220 V at the low voltage side, while HV windings are open circuited, i.e. CB2 is open (Figure 6a). For the purpose of checking the operation of the algorithm when CT saturation at the LV side is present, phases A, B, and C contain 2 CTs connected in series with different burdens at the secondary side. Current transformers CT_{LV-A}, CT_{LV-B}, and CT_{LV-C} have identical characteristics and during the experiment they have accurately reproduced currents to the secondary side. On the other hand, current transformers CT_{A-S}, CT_{B-S}, and CT_{C-S}, also having identical characteristics, are chosen so that they go to saturation during the experiment.

A 5 kHz sampling frequency was selected. From the CT's secondary, the following 7 adapted signals are fed to the input of DAQ NI USB 6009: 1) currents of phase A - CT_{LV-A} and CT_{A-S} , 2) currents of phase B - CT_{LV-B} and CT_{B-S}, 3) currents of phase C - CT_{LV-C} and CT_{C-S}, and 4) current of the transformer neutral CT_{LV-N}.

Since the value and waveform of the magnetizing current are of a random nature, the energization experiment was repeated several times. Figure 7 shows phase currents with and without CT saturation for 1 case of energization that was recorded during the experiment. Figure 8a shows the difference of currents $3i_0$ and i_G when CT saturation was not taken into account (i_{0diff}) and when saturation of all 3 phase CTs was taken into account ($i_{0diff-sat}$). It can be noted that in the case of CT saturation a significant value of zero differential current appears. Figure 8b shows the characteristic of a conventional REF relay that, as the restraint current, uses the sum of $3I_0$ and I_G [2]. The relay characteristic slope is 25% and pick-up current is 0.2 pu. It can be noted from the figure that in the case of saturated phase CTs the calculated current trajectory enters the operation area. In this case the conventional differential type of REF relay would operate unnecessarily.

On the other hand, in the studies shown in Figure 9a, operation of the presented algorithm was tested during a magnetizing inrush, when CTs did not go to saturation (case 1). This figure shows the directional indicator response. Moreover, it can be noted that without CT saturation, the directional index reaches values close to 1 pu within 5 ms and consequently the trip signal is not activated. Figure 9b shows the measured currents of the transformer neutral CT and calculated sums of the phase currents in the case when CTs did go to saturation. All values of the index shown in Figure 9b are outside the relay operation area; therefore the relay based on the method presented in this paper would not trip unnecessarily.

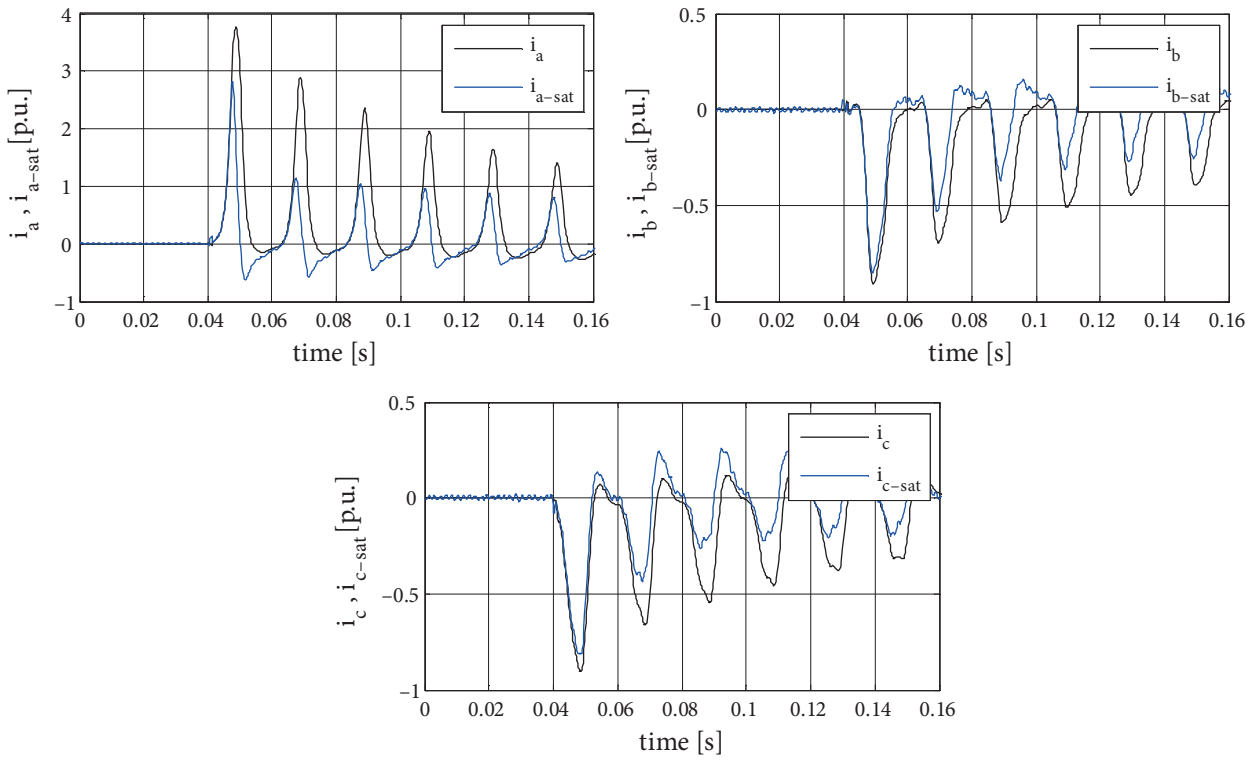

Figure 7. Phase currents with and without current transformer saturation.

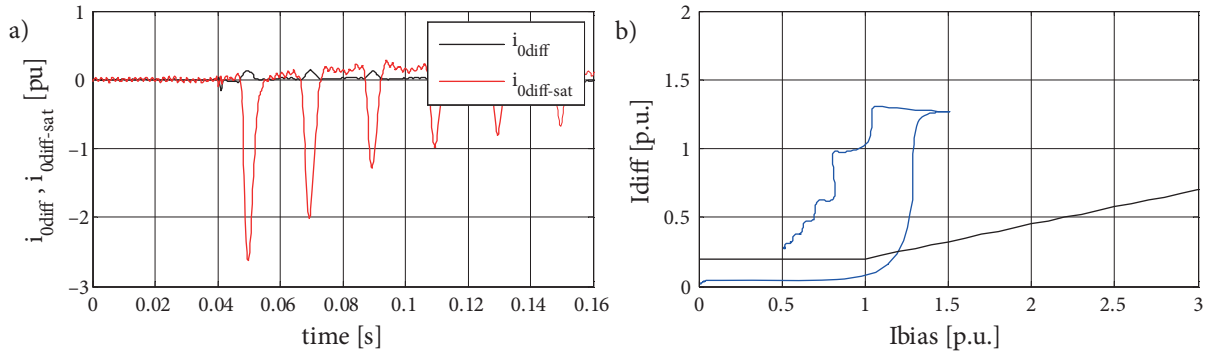

Figure 8. a) Zero sequence differential current; b) calculated current trajectory in case of current transformer saturation based on the modelled conventional relay.

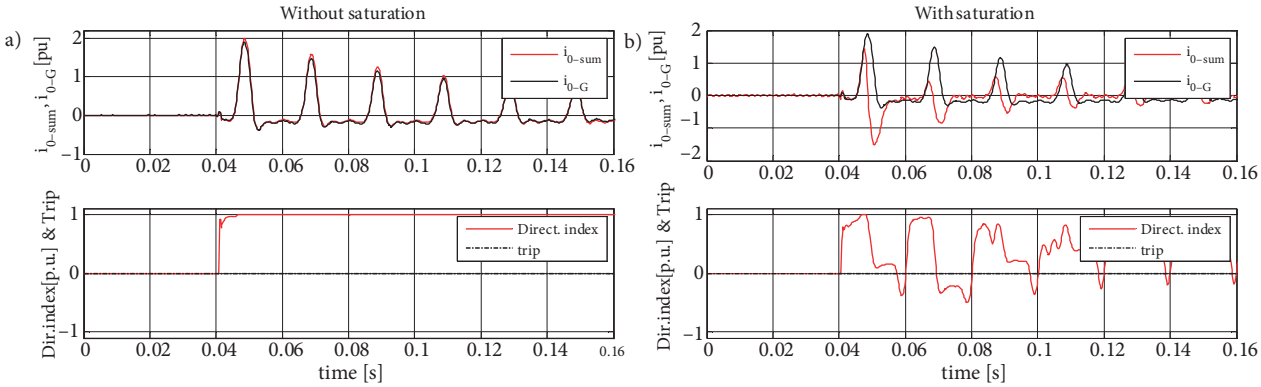

Figure 9. Currents i_{0_sum} and i_{0_G}, index I_{DI} and trip decision: a) case 1; b) case 2.

3.2. Energization with internal fault

Operation of the algorithm during switching on of a transformer having a phase-to-ground fault in phase A was tested through examples 3 to 9. Phase-to-ground faults between the selected tap on the HV transformer winding and ground were realized manually, and then the energization of the faulty transformer was activated by closing CB1. Energization tests of the unladen faulty transformer were divided into 2 groups. In the first group, examples 3 to 5, the faulty transformer was fed from the HV side while terminals at the LV side were open (Figure 6b), and the fault in the winding was at the feeding side. From the CTs secondary, the following 4 adapted signals were observed: HV phase currents CT_{HV-A}, CT_{HV-B}, CT_{HV-C}, and the current of the transformer neutral CT_{HV-N}. Figure 10 shows the sum of the phase currents and the neutral current for a turn-to-ground fault located at 25% from the neutral winding end of phase A (case 3). The operating response of the corresponding directional indicator shows the presence of an internal fault and the trip signal is activated approximately 1 ms after the fault occurrence.

In the second group, examples 6 to 9, faults were generated in the HV winding while the transformer was fed from the LV side (Figure 6a). Therefore, a fault was generated at the transformer side having open terminals. From the CTs secondary, the following 8 adapted signals were observed: HV phase currents: CT_{HV-A}, CT_{HV-B}, CT_{HV-C}; LV phase currents: CT_{LV-A}, CT_{LV-B}, CT_{LV-C}; and currents of the transformer neutrals: CT_{HV-N} and CT_{LV-N}. Figure 11 shows the results obtained for case 6. In this case a turn-to-ground fault was located at 25% from the neutral HV winding end of phase A. For the REF unit of the LV

winding (Figure 11a), the fault is external, which was recognized by the algorithm. In this case, the LV side trip signal was not activated. The logic of recognizing a fault in the HV winding is quite simple. If the sum of the phase currents is equal to zero and a current flows through the neutral conductor that is higher than the preassigned limiting value, it is clear that a phase-to-ground fault is present and the transformer should be switched off. In the considered case, as expected, the REF unit of the HV winding where the fault was located tripped (Figure 11b).

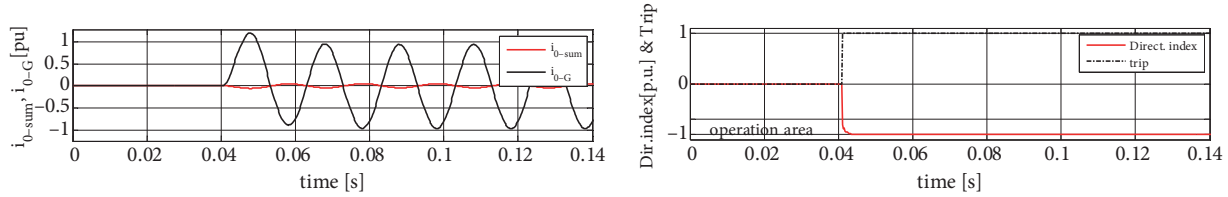

Figure 10. Algorithm performance for HV side for case 3: energization from high voltage side, ground fault on high voltage winding.

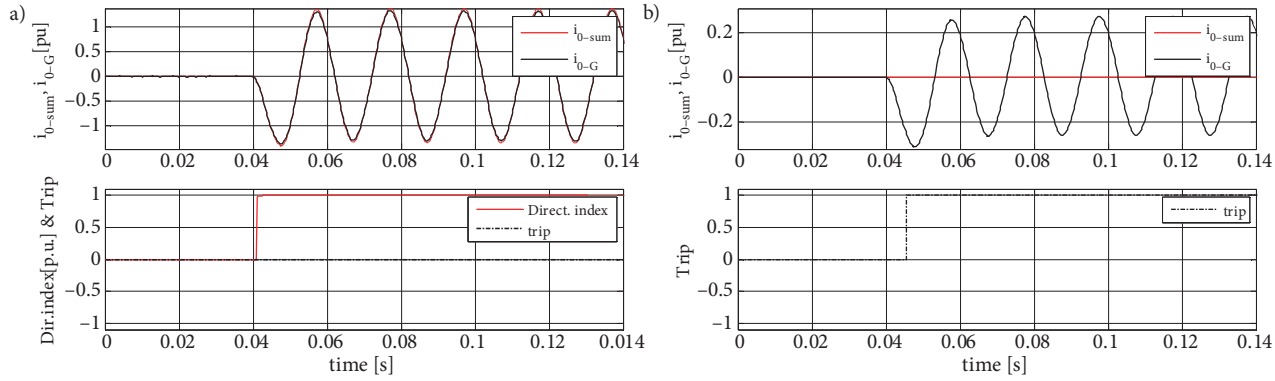

Figure 11. Case 6: energization from low voltage side of a faulty transformer, ground fault in the high voltage winding - algorithm performance for: a) low voltage side, b) high voltage side.

3.3. Internal and external faults of a loaded transformer

The operation of the algorithm during internal faults was tested by cases 10 to 15. The examples covered internal faults accompanied by CT saturation: saturation of the phase CT located in the phase hit by the fault (case 14) and saturation of the neutral CT (case 15). In cases 16 to 18 the algorithm was tested during external faults. Here also, CT saturation and its influence on operation of the algorithm were taken into account. Figure 5 shows the circuit diagram used for these measurements. Both breakers CB1 and CB2 were closed during experiments. Directional indicators for cases 10 to 18 are shown in Figure 12. In all these cases the fault occurred at $t=$ 40 ms. All detectors clearly discriminated the occurred faults. The time needed for activation of trip signal in the presence of fault is given in Table 2.

Table 2. Internal fault – instant of activation of trip signal

Case	10	11	12	13	14	15
t [ms]	1	1.8	1.8	0.8	0.4	1.2

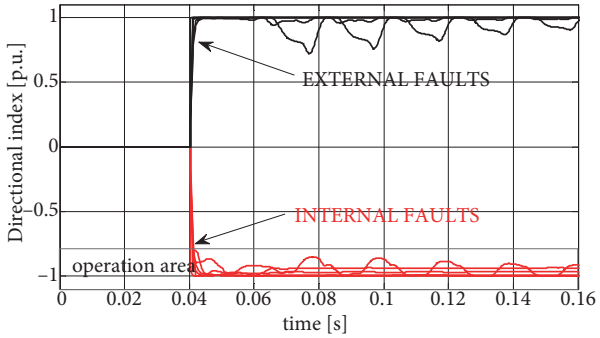

Figure 12. Directional index for external and internal faults of loaded transformer.

3.4. Additional enhancement of algorithm performance

Testing of the algorithm showed that its application could avoid unnecessary tripping of REF protection caused by CT saturation. Figure 9b shows that the value of the directional index oscillates in the case of energization of an unladen transformer in conjunction with CT saturation. The figure clearly shows that the directional index takes negative values, but remains predominantly positive. It can be noted that the period of oscillations of the index is approximately equal to the period of the signal. Thus averaging the index over 1 period of the signal could eliminate, or significantly reduce, oscillations of the index, as will be shown. By averaging, values of the index will be shifted away from the operation area. In this way, the reliability of the algorithm in the cases of deeper CT saturations would be additionally enhanced. From the point of view of reducing the operational delay of the algorithm, in what follows the behavior of the index for averaging over half periods will be checked. At first, it is required to form the vector in which the last n values of index I_{DI} will be stored:

$$\left[\; I_{DI}(1) \quad I_{DI}(2) \quad I_{DI}(3) \quad \ldots \quad I_{DI}(n-1) \quad I_{DI}(n) \;\right], \tag{10}$$

The average value is calculated by the expression

$$I_{DI-avg}(k) = \frac{1}{n}\sum_{i=1}^{n} I_{DI}(i), \tag{11}$$

where n = m/2, if averaging is performed over 1 half of the period, or n = m if averaging is performed over 1 full period. Figures 13a and 13b show the averaged values of the directional index from cases 1 and 2, respectively.

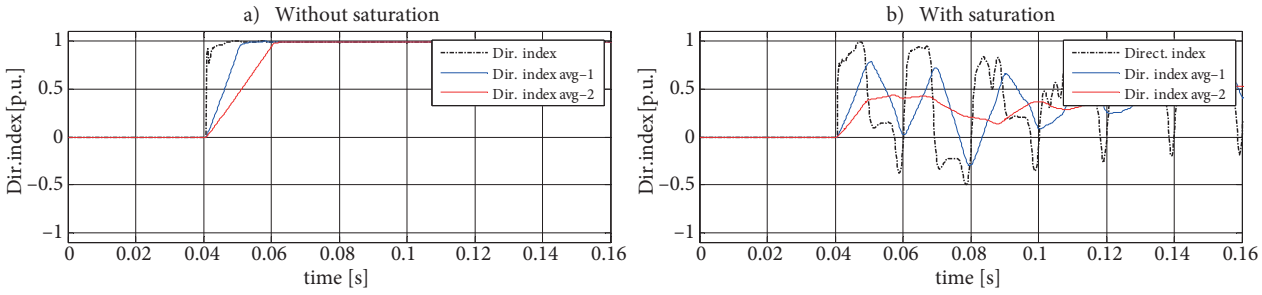

Figure 13. Averaged directional indexes over 1 half and over a full period of the signal (a) case 1, (b) case 2.

In the course of taking decisions, the algorithm makes use of the directional index value (equation 4). For the purpose of making the effect of averaging obvious, the phase shift between i_0 and i_G was estimated by

using the expressions

$$\phi_{DI} = \arccos(I_{DI}) \phi_{DI-avg\,T/2} = \arccos(I_{DI-avg\,T/2}) \phi_{DI-avg\,T} = \arccos(I_{DI-avg\,T}), \tag{12}$$

where φ_{DI}, $\varphi_{DI-avg\,T/2}$, and $\varphi_{DI-avg\,T}$ – estimated the values of phase shift on the basis of directional index (I_{DI}), averaged value of the index over half period ($\mathrm{I}_{DI-avg\,T/2}$), and over full period ($\mathrm{I}_{DI-avg\,T}$). Trajectories of the estimated phase shifts φ_{DI} (Figure 14a), $\varphi_{DI-avg\ T/2}$ (Figure 14b), and $\varphi_{DI-avg\,T}$ (Figure 14c) are shown on the tripping characteristic for all examples from Table 1.

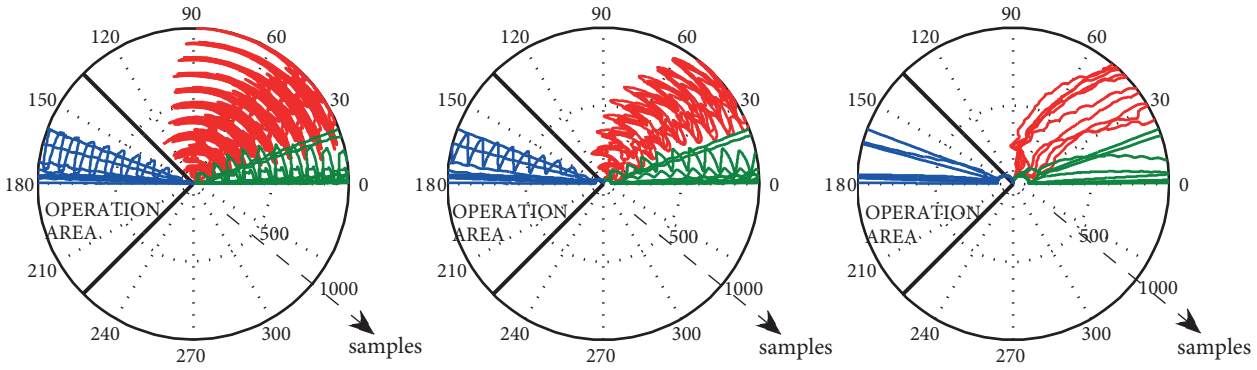

Figure 14. Trajectories of the phase shift: a) φ_{DI}, b) $\varphi_{DI-avg\,T/2}$, c) $\varphi_{DI-avg\,T}$.

Table 3 shows the time needed for the activation of the trip signal in cases of internal faults. Instants of relay operation are given in the table, when for making the trip decision the relay makes use of the directional index averaged over half of the period ($\mathrm{I}_{DI-avg\,T/2}$) or over a full period ($\mathrm{I}_{DI-avg\,T}$).

Table 3. Instant of activation of trip signal (by using I_{DI} , $\mathrm{I}_{DI-avg\,T/2}$, and $\mathrm{I}_{DI-avg\,T}$).

Case	3	4	5	10	11	12	13	14	15
	t (ms)								
I_{DI}	1	0.8	0.6	1	1.8	1.8	0.8	0.4	1.2
$\mathrm{I}_{DI-avg\,T/2}$	8.2	7.8	7.6	8	8.8	9.2	8.6	7.4	8
$\mathrm{I}_{DI-avg\,T}$	15.2	14.8	14.8	15.2	16	16.2	15.8	14.8	15

From the presented results it is clear that by application of the new algorithm the unnecessary operations during magnetizing inrush in conjunction with CT saturation would be avoided, thereby the REF protection of transformers is improved. The application of averaged values would increase the reliability of relay operation in cases of deep CT saturations. Averaging over half of the period noticeably reduces oscillations of the directional index, which is used for making the trip decision. From Table 3, it can be seen that at internal faults, application of index $\mathrm{I}_{DI-avg\,T/2}$ would activate trip signal within 10 ms. It was shown that averaging over a full period results in the best stability of directional index value $\mathrm{I}_{DI-avg\,T}$, and that by application of this index an internal fault is recognized within 17 ms in all cases.

4. Influence on operation of the algorithm of different levels of CT saturation

As already mentioned, CT saturation is difficult to predict. A CT may enter saturation due to different reasons, among them high amplitude of fault current, presence of the DC component, and remanent flux in CT core.

In this section, the influence on operation of the algorithm of different levels of CT saturation due to different remanent fluxes in CT cores is investigated. By applying MATLAB module Power Systems Blockset, the CT of characteristics corresponding to CT_{A-S}, CT_{B-S}, and CT_{C-S} from case 2 is modelled (see Figure 15), and then its operation is simulated. In the presented model, the primary of CT, via a controlled current source (CCS), is fed by samples of the laboratory recorded signals of the transformer's magnetizing inrush current. The signals were fed to the CT model whose remanent flux was varied. Figure 16 shows the laboratory recorded waveforms of phase currents for 10 switch-ons of the unloaded power transformer which were used as inputs to the model. The signals of the phase currents and neutral current are recorded according to the circuit diagram of Figure 6a.

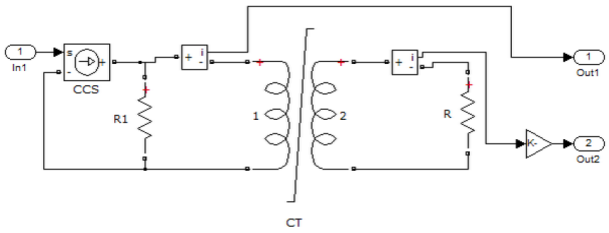

Figure 15. Current transformer simulation model.

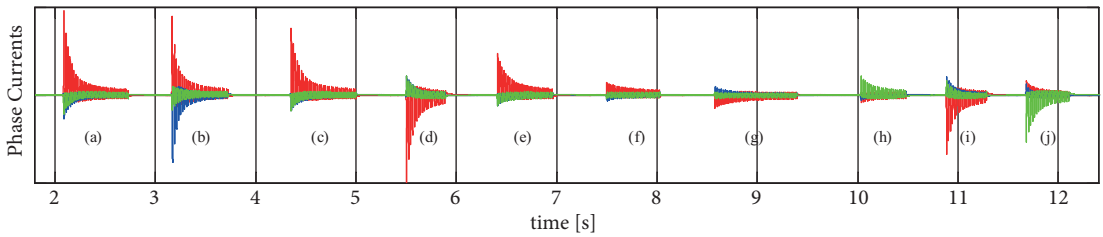

Figure 16. Phase currents during switch-on of an unloaded power transformer.

During these investigations it was assumed that only phase CTs enter saturation, while the neutral CT correctly transfers the current through the model. For all examples, (a) to (j), each phase current is fed to the CT model. By means of the obtained CT secondary currents, the sum of phase currents ($3i_0$) was calculated and then compared to the measured current of the neutral conductor (i_G). Operation of the conventional REF relay and the proposed algorithm was tested. In the simulations of CT operation, the remanent fluxes were modelled by remanent flux amplitude and a parameter that identifies the flux pattern [36,37]. The remanent flux amplitude was varied from -80% to 80% of the rated flux. The remanent flux patterns were modelled as $\{\Psi_0, -\Psi_0, 0\}$ in all the possible phase permutations. Figures 17a, 17b, and 18 show the obtained results for 1 remanent flux pattern. Moreover, it should be borne in mind that CT_{A-S}, CT_{B-S}, and CT_{C-S} from case 2 were underrated. Therefore, even at 0% of the remanent flux they went to saturation.

Figure 17a shows trip decisions and time instants of activation of the trip signal in the cases when the algorithm of a conventional type of REF relay operated unnecessarily. The relay characteristic slope is 25% and pick up current is 0.2 pu. Figure 17b shows maximum values of the estimated phase shifts during the first 4 periods upon switch-on of the transformer. It can be noted that all phase shifts were outside the operation area and that the new algorithm would not have operated. Figures 18a and 18b show maximum values of the estimated phase shifts $\varphi_{DI-avgT/2}$ and $\varphi_{DI-avgT}$ during the first 4 periods upon switch-on of the transformer

obtained on the basis of averaged directional index. From this figure it can also be noted that averaging of the directional index results in shifting away from the operation area.

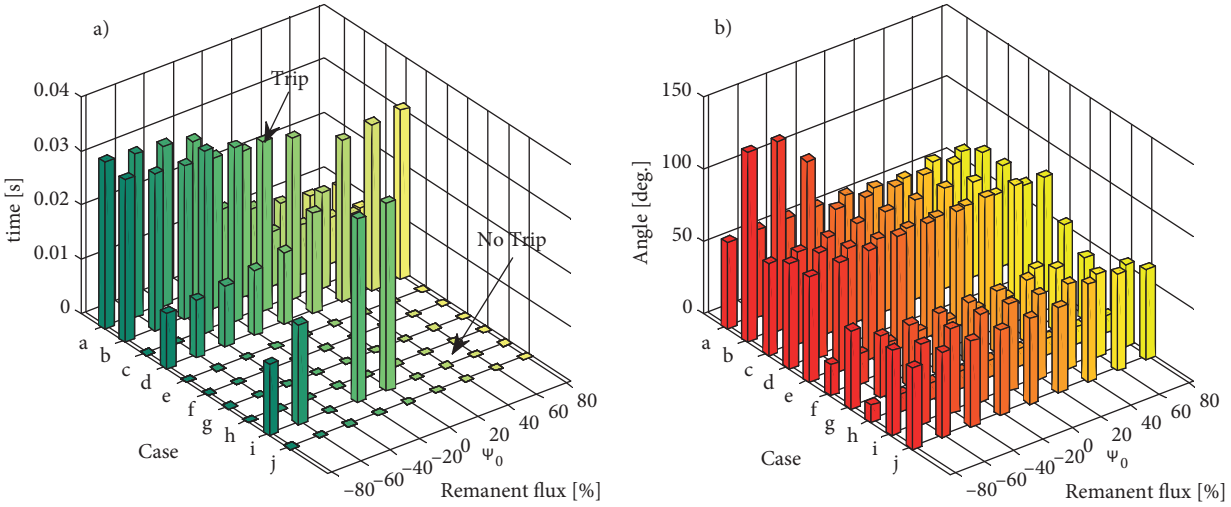

Figure 17. a) Trip decision and time instant of (unnecessary) operation of conventional REF relay; b) Maximum values of estimated phase shift by the new algorithm.

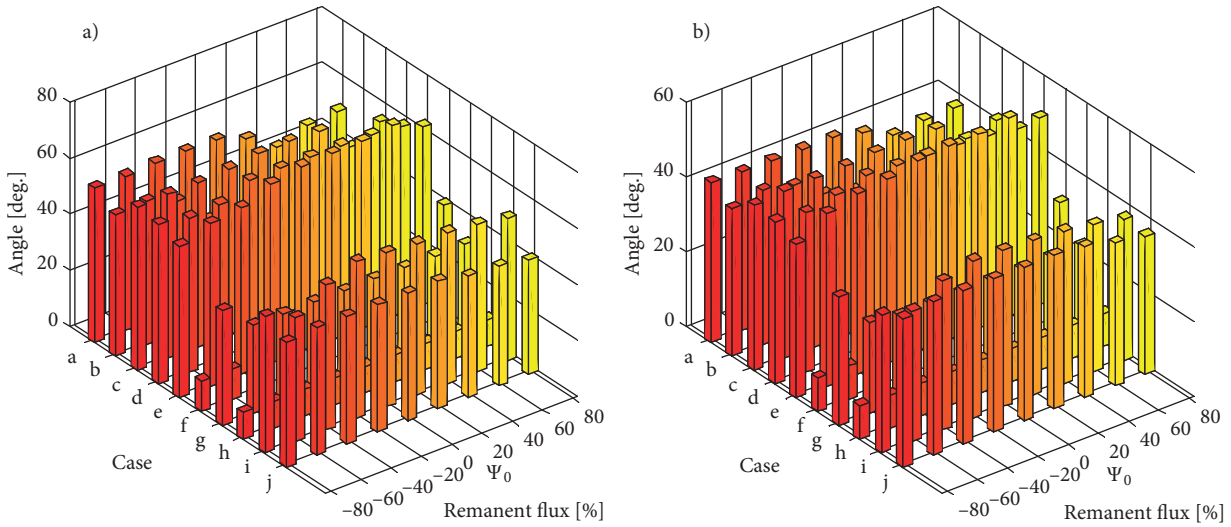

Figure 18. Maximum values of estimated phase shifts a) $\varphi_{DI-avgT/2}$, b) $\varphi_{DI-avgT}$.

5. Definite block judgement

On the basis of the performance of the proposed algorithm during tests presented in sections 3 and 4, definite tripping characteristics, shown in Figure 19a, can be formulated. In accordance with this, in the algorithm presented in subsection 2.3 the discrimination stage can be modified (Figure 19b). For discrimination performance a register (equation 10) needs to be formed for storing the last n values of the directional index. The proposed algorithm (subsection 2.3) during step 6 checks the value of the directional index:

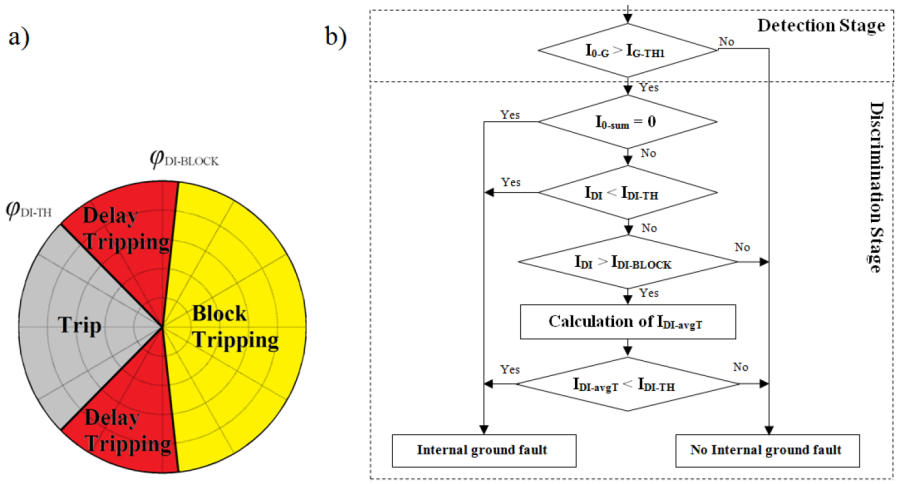

Figure 19. a) Definite tripping characteristic; b) modification of discrimination stage.

If condition $I_{DI} < I_{DI\_TH}$ is satisfied, it is necessary that the relay operates. If the condition is not satisfied, additional checking of directional index value is introduced in the following way:

- If the value of the index is higher than the adjusted value I_{DI_BLOCK} $(I_{DI} > I_{DI\_BLOCK})$ operation of the relay is blocked.

- If the value of the index satisfies the following relation: $I_{DI\_TH} \leq I_{DI} \leq I_{DI\_BLOCK}$, the algorithm, by using the values stored in the register (equation 10) and expression (11), calculates the value of the directional index averaged over a full period $(I_{DI-avgT})$. Then, if condition $I_{DI-avgT} < I_{DI\_TH}$ is satisfied, the presence of an internal fault is assumed and the relay trips.

6. Conclusion

The influence of magnetizing inrush and CT saturation on restricted earth fault protection was considered. An enhanced algorithm based on a time-domain digital phase comparator was proposed. The implementation of the proposed algorithm would prevent false REF relay tripping and provide proper operation during energization of the transformer.

The directional index calculated over 1 half period of the signal was used for digital phase comparison. This ensures a high speed response of the algorithm. Additional enhancement of the algorithm performance by averaging the values of the directional index was also achieved. At deep CT saturations during magnetizing inrush oscillations of the index value are reduced by averaging and shifted away from the operation area. In this way, high stability and security of the algorithm performance is provided. The new method does not use blocking in terms of the second harmonic, which results in a high speed and reliability of making trip decision during energization of a faulty transformer.

The algorithm was tested by a number of energization and fault cases recorded in the laboratory and by simulations of CT operation during initial transformer energization. Based on the experimental and simulation results, the new algorithm is verified to be applicable under conditions of magnetizing inrush and CT saturation.

Acknowledgment

The authors would like to thank the Ministry of Science and Technological Development of the Republic of Serbia (project III 42009), which made this work possible.

References

[1] Sezi T. A new approach for transformer ground differential protection. In: Industrial and Commercial Power Systems Technical Conference; 11–16 Apr 1999; New Orleans, LA, USA. New York, NY, USA: IEEE. pp. 394-399.

[2] IEEE Standard C37.91. IEEE Guide for Protective Relay Applications to Power Transformers. New York, NY, USA: IEEE, 2008.

[3] Cosse RE, Nichols WH. The practice of ground differential relaying. IEEE T Ind Appl 1994; 30: 1472-1479.

[4] Stringer D. Ground differential protection: revisited. In: Industrial and Commercial Power Systems Technical Conference; 2–6 May 1999; Sparks, NV, USA: IEEE. pp. 1-8.

[5] Sutherland PE. Application of transformer ground differential protection relays. IEEE T Ind Appl 2000; 36: 16-21.

[6] Rockefeller GD. Fault protection with a digital computer. IEEE T Power Ap Syst 1969; 88: 438-464.

[7] Youssef OAS. A wavelet-based technique for discrimination between faults and magnetizing inrush currents in transformers. IEEE T Power Deliver 2003; 18: 170-176.

[8] Saleh SA, Rahman MA. Modeling and protection of a three-phase transformer using wavelet packet transform. IEEE T Power Deliver 2005; 20: 1273-1282.

[9] Ozgonenel O, Onbilgin G, Kocaman C. Transformer protection using the wavelet transform. Turk J Elec Eng & Comp Sci 2005; 13: 119-135.

[10] Pihler J, Grcar B, Dolinar D. Improved operation of power transformer protection using artificial neural network. IEEE T Power Deliver 1997; 12: 1128-1136.

[11] Tripathy M. Power transformer differential protection using neural network principal component analysis and radial basis function neural network. Simul Model Pract Th 2010; 18: 600-611.

[12] Perez LG, Flechsig AJ, Meador JL, Obradovic Z. Training an artificial neural network to discriminate between magnetizing inrush and internal faults. IEEE T Power Deliver 1994; 9: 434-441.

[13] Kılıç E, Özgönenel O, Usta Ö, Thomas D. PCA based protection algorithm for transformer internal faults. Turk J Elec Eng & Comp Sci 2009; 17: 125–142.

[14] Khorashadi-Zadeh H, Li Z. A sensitive ANN based differential relay for transformer protection with security against CT saturation and tap changer operation. Turk J Elec Eng & Comp Sci 2007; 15: 351-368.

[15] Wiszniewski A, Kasztenny B. A multi-criteria differential transformer relay based on fuzzy logic. IEEE T Power Deliver 1995; 10: 1786-1792.

[16] Shin MC, Park CW, Kim JH. Fuzzy logic-based relaying for large power transformer protection. IEEE T Power Deliver 2003; 18: 718-724.

[17] Ashrafian A, Rostami M, Gharehpetian GB. Characterization of internal disturbances and external faults in transformers using an S-transform–based algorithm. Turk J Elec Eng & Comp Sci 2013; 21: 330-349.

[18] Jia S, Wang S, Zheng G. A new approach to identify inrush current based on generalized S-transform. In: International Conference on Electrical Machines and Systems; 17–20 Oct 2008; Wuhan, China. New York, NY, USA: IEEE. pp. 4317-4322.

[19] Guzmán A, Zocholl S, Benmouyal G, Altuve H. A current-based solution for transformer differential protection – Part I: Problem statement. IEEE T Power Deliver 2001; 16: 485-491.

[20] Rahman MA, Jeyasurya B. A state-of-the-art review of transformer protection algorithms. IEEE T Power Deliver 1988; 3: 534-544.

[21] Sharp RL, Glassburn WE. A transformer differential relay with second-harmonic restraint. IEEE T Power Ap Syst 1958; 77: 913-918.

[22] IEEE Power Engineering Society. Transient response of current transformers. IEEE T Power Ap Syst 1977; 96: 1809-1814.

[23] IEEE Standard C37.110. IEEE Guide for the Application of Current Transformers Used for Protective Relaying Purposes. New York, NY, USA: IEEE, 2008.

[24] Wentz EC, Sonnemann WK. Current transformers and relays for high-speed differential protection, with particular reference to offset transient currents. Electr Eng 1940; 59: 481-488.

[25] Guzmán A, Altuve HJ, Benmouyal G. Power Transformer Protection. In: James H. Harlow, editor. Electric Power Transformer Engineering. Boca Raton, FL, USA: CRC Press, 2004. pp. 353-381.

[26] Hunt R. Impact of CT errors on protective relays – case studies and analysis. IEEE T Ind Appl 2011; 48: 52-61.

[27] Labuschagne C, Merwe IV, Enterprises E. A comparison between high-impedance and low-impedance restricted earth-fault transformer protection. Tech Pap Schweitzer Eng Labs 2007; 1: 1-9.

[28] Kasztenny B. Impact of transformer inrush currents on sensitive protection functions How to configure adjacent relays to avoid nuisance tripping. In: 59th Annual Conference for Protective Relay Engineers; 4–6 April 2006, College Station, TX, USA. New York, NY, USA: IEEE. pp. 103-123.

[29] Krstivojevic J, Djurić M. A new method of improving transformer restricted earth fault protection. Adv Electr Comput En 2014; 14: 41-48.

[30] Davarpanah M, Sanaye-Pasand M, Iravani R. Performance enhancement of the transformer restricted earth fault relay. IEEE T Power Deliver 2013; 28: 467-474.

[31] Stojanović Z, Djurić M. The algorithm for directional element without dead tripping zone based on digital phase comparator. Electr Pow Syst Res 2011; 81: 377-383.

[32] Elmore W. Protective Relaying Theory and Applications. 2nd ed. Boca Raton, FL, USA: CRC Press, 2004.

[33] Liu P, Malik OP, Chen D; Hope GS, Guo Y. Improved operation of differential protection of power transformers for internal faults. IEEE T Power Deliver 1992; 7: 1912-1919.

[34] Zubić S, Djurić M. A distance relay algorithm based on the phase comparison principle. Electr Pow Syst Res 2012; 92: 20-28.

[35] Stojanović Z, Djurić M. An algorithm for directional earth-fault relay with no voltage inputs. Electr Pow Syst Res 2013; 96: 144-149.

[36] Brunke JH, Fröhlich KJ. Elimination of transformer inrush currents by controlled switching – Part I: Theoretical considerations. IEEE T Power Deliver 2001; 16: 276-280.

[37] Duro MM, Denis R. Parameter uncertainty assessment in the calculation of the overvoltages due to transformer energization in resonant networks. In: CIGRE 2012; 26–31 Aug 2012; Paris, France. CIGRE 2012: C4-204. pp. 1-12.